

Scientific paper

# New Mg-based 4,4'-biphenyldicarboxylate Coordination Polymer with Layered Crystal Structure

Matjaž Mazaj,<sup>1,\*</sup> Marta Kasunič,<sup>2</sup> Venčeslav Kaučič<sup>1,3</sup>  
and Nataša Zabukovec Logar<sup>1,3</sup>

<sup>1</sup> National Institute of Chemistry, Hajdrihova 19, 1000 Ljubljana, Slovenia

<sup>2</sup> University of Ljubljana, Faculty of Chemistry and Chemical Technology, Aškerčeva 5, 1000 Ljubljana, Slovenia

<sup>3</sup> CO-NOT Centre of Excellence, Hajdrihova 19, 1000 Ljubljana, Slovenia

\* Corresponding author: E-mail: matjaz.mazaj@ki.si

Received: 01-10-2013

Dedicated to the memory of Prof. Dr. Marija Kosec.

## Abstract

New magnesium 4,4'-biphenyldicarboxylate (BPDC) was solvothermally synthesized in the presence of *N,N'*-dimethylformamide (DMF). The crystal structure with formula  $\text{Mg}_3(\text{BPDC})_3(\text{DMF})_4$  and denoted as NICS-7 was solved in monoclinic symmetry with space group *Pn* (no. 7) and unit cell parameters  $a = 12.6433(7)$  Å,  $b = 13.3950(5)$  Å,  $c = 19.9230(8)$  Å,  $\beta = 107.131(5)^\circ$ . The structure consists of  $\text{MgO}_6$  linear arranged trimers with common vertices connected through BPDC ligands forming extended 2-dimensional layered hybrid structure. Each terminal Mg atom within trimeric clusters is coordinated by two dimethylformamide molecules, respectively. Layers of  $\text{Mg}_3(\text{BPDC})_3(\text{DMF})_4$  are stabilized by non-coordinated dimethylformamide molecules located within the voids in crystallographically disordered manner. Thermal properties of NICS-7 were determined by thermogravimetric and temperature-programmed X-ray diffraction. The structure remains stable only up to 50 °C. At higher temperatures, the removal of non-coordinated dimethylformamide molecules causes formation of amorphous Mg-BPDC phase.

**Keywords:** Metal-organic framework, magnesium 4,4'-biphenyldicarboxylate, Mg-trimeric SBU

## 1. Introduction

Hybrid organic-inorganic coordination polymers or metal organic frameworks (MOFs) represent extensive group of materials where inorganic building units are interconnected through organic ligands forming crystalline structure. MOF materials may exhibit highly porous 3-dimensional frameworks enabling promising applications in various fields such as separation, catalysis, drug delivery and electrochemistry.<sup>1–5</sup> Due to the ability to control their pore dimensions by proper choice of synthesis parameters and possibility to generate preferential sorption sites within the framework, MOF materials are most widely explored for gas storage applications.<sup>6–11</sup> One of the prerequisites for effective gas storage with high w/w uptake capacities is low density framework, which can be achieved by production of MOFs based on light-weight metals such as magnesium or

aluminium. In contrast with rapidly increasing research on transition metal-based MOF materials resulting in numerous newly discovered structures published every year, magnesium-based coordination polymers are relatively unexplored. Studies of Mg-based coordination polymers formation were performed using aliphatic carboxylic acids such as formic, squaric, diglycolic, glutaric, sebacic, cyclobutanetetracarboxylic and camphoric acid as ligands.<sup>12–16</sup> However, more frequently used ligands included in exploration of new Mg-MOF materials represent aromatic polycarboxylates, that could provide frameworks with permanent porosity due to their molecule rigidities. Among all known Mg-based polycarboxylate structures, only few of them exhibit permanent porosity and accessibility for gas molecules due to the relatively limited knowledge about their crystallization processes.<sup>12,17–26</sup> Formation of Mg-based 1,4-benzenedicarboxylates, 2,6-naphthalenedicarboxylates, 3,5-pyridinedicar-

boxylates and 1,3,5-benzenetricarboxylates were already systematically studied varying different synthesis parameters,<sup>27–31</sup> however in order to gain more knowledge about the chemistry of Mg-based open framework structures formation, further studies in this field are still required.

4,4'-biphenyldicarboxylic acid (BPDC) represents alternative ligand in crystal engineering of isorecticular 1,4-benzenedicarboxylate-based (BDC) MOFs, forming larger pores in comparison with BDC-based MOFs. Coordination networks with BPDC and DMF are quite common and well studied, especially when containing transition metal centers. However, only few structures with magnesium and aforementioned organic molecules were described till now.<sup>24,32,33</sup> In that manner we describe the synthesis, crystal structure and thermal properties of a new layered Mg-4,4'-biphenyldicarboxylate, Mg<sub>3</sub>(BPDC)<sub>3</sub>(DMF)<sub>4</sub> denoted as NICS-7 (NICS = National Institute of Chemistry Slovenia).

## 2. Experimental

### 2. 1. Synthesis of NICS-7

In typical synthesis 0.26 g (1.07 mmol) of 4,4'-biphenyldicarboxylic acid (97% BPDC, Sigma-Aldrich) was dispersed in 30 ml of *N,N'*-dimethylformamide (99.8% DMF, Sigma-Aldrich) in glass vial. Subsequently 0.36 g (1.4 mmol) of Mg(NO<sub>3</sub>)<sub>2</sub> · 6H<sub>2</sub>O was added. Sealed vial was heated to 120 °C. Plate-like crystals of NICS-7, formed after 24 hours of hydrothermal treatment, were recovered by filtration and drying in vacuum at room temperature. Elemental analysis yielded the values of 6.8 wt.% Mg, 63.4 wt.% C, 6.3 wt.% N, 23.5 wt. % O which are in agreement with the theoretical values (6.6 wt.% Mg, 62.2 wt.% C, 6.4 wt.% N, 24.7 wt. % O).

### 2. 2. Single-crystal Structure Analysis

The proper single crystal of NICS-7 was mounted on the tip of glass fibre with a small amount of silicon grease and transferred to a goniometer head. Data were collected on a Agilent SuperNova (Dual, Cu at zero, Atlas) diffractometer using Mo K $\alpha$  radiation at 150 K. Data reduction and integration were performed with the software package *CrysAlis PRO*.<sup>34</sup> The coordinates of non-hydrogen atoms were found *via* direct methods using the structure solution program *SIR97*.<sup>35</sup> A full-matrix least-squares refinement on  $F^2$  magnitudes with anisotropic displacement parameters for all non-hydrogen atoms using *SHELXL-97* was employed.<sup>36</sup> All hydrogen atoms were initially located in difference Fourier maps. However, they were subsequently treated as riding atoms at geometrically idealized positions with bond lengths C–H of 0.98 Å for methyl and 0.95 Å for aromatic C–H bonds. The corresponding displacement parameters  $U_{iso}(H)$  were 1.5-times higher than those of the carrier methyl carbons and 1.2-times higher than all other hydrogen bearing carbon atoms.

The *N,N*-dimethylformamide molecules, occupying the cavities in the crystal structure, are highly disordered and could not be modelled successfully. Consequently, their scattering contribution was removed from the refinement using the *SQUEEZE* routine in the program *PLATON*<sup>37</sup> which gave solvent-accessible voids of ca. 225 Å<sup>3</sup> for only 26 electrons. Figures depicting the structures were prepared by *ORTEP3*.<sup>38</sup> Crystal data and information on data collection and refinement are given in Table 1.

CCDC-960675 contains the supplementary crystallographic data for this paper. These data can be obtained free of charge from The Cambridge Crystallographic Data Centre *via* [www.ccdc.cam.ac.uk/data\\_request/cif](http://www.ccdc.cam.ac.uk/data_request/cif).

**Table 1.** Crystal data, data collection and structure refinement for the title compound.

Crystal data	
Formula	C <sub>57</sub> H <sub>59</sub> Mg <sub>3</sub> N <sub>5</sub> O <sub>17</sub>
Mr	1159.02
Cell setting, space group	Monoclinic, <i>P</i> 1 <i>n</i> 1
<i>a</i> (Å)	12.6433(7)
<i>b</i> (Å)	13.3950(5)
<i>c</i> (Å)	19.9230(8)
$\beta$ (°)	107.131(5)
<i>V</i> (Å <sup>3</sup> )	3224.4(3)
<i>Z</i>	2
$D_x$ (Mg m <sup>-3</sup> )	1.194
$\mu$ (mm <sup>-1</sup> )	0.114
<i>F</i> (000)	1216
Crystal form, colour	prism, colourless
Crystal size (mm)	0.35 × 0.25 × 0.20
Data collection	
Temperature (K)	150
Radiation type, wavelength	Mo K $\alpha$ , 0.71073 Å
Diffractometer	Agilent SuperNova (Dual, Cu at zero, Atlas)
Data collection method	$\omega$ scans
Absorption correction	multi-scan
No. of measured, independent and observed reflections	19236, 11941, 8838
Criterion for observed reflections	$F^2 > 2.0 \sigma(F^2)$
$R_{int}$	0.0387
$\theta$ range (°)	3.04–27.28
<i>h</i> range	–1615
<i>k</i> range	–1717
<i>l</i> range	–2425
Refinement	
Refinement method	full matrix least-squares on $F^2$
$R$ (on $F_{obs}$ ), $wR$ (on $F_{obs}$ ), $S$	0.0686, 0.179, 1.008
No. of contributing reflections	11941
No. of parameters	749
No. of restraints	2
H-atom treatment	observed in difference Fourier map and refined as riding
$(\Delta\sigma)_{max}$ , $(\Delta\sigma)_{ave}$	<0.001, <0.001
$\Delta\rho_{max}$ , $\Delta\rho_{min}$ (eÅ <sup>-3</sup> )	0.495, –0.294

## 2. 3. Characterization Methods

Elemental analysis was performed by energy dispersive X-ray analysis (EDX). In order to approximate the bulk analysis, the sample was grinded and compressed to self-supported pellet. EDX mapping analysis was performed on even surface of the pellet with area of about 0.2 mm<sup>2</sup> on a Zeiss Supra 3VP field-emission scanning electron microscope equipped with INCA Energy system. Fourier-transform infra-red (FT-IR) measurements were performed on a Perkin Elmer Spectrum One FTIR spectrometer with resolution of 1 cm<sup>-1</sup> from self-supporting KBr pellets. Thermogravimetric (TG/DTG) analysis was performed on a SDT 2960 Thermal Analysis System (TA Instruments, Inc.). The measurement was carried out in static air with the heating rate of 10 °C · min<sup>-1</sup>. Thermal stability of NICS-7 material was monitored by high-temperature XRD measurements in air flow using a PANalytical X'Pert PRO MPD diffractometer with CuK<sub>α1</sub> wavelength from 5 to 60° 2θ using step of 0.039° with collection time 100 s per step in the temperature range between 25 and 400 °C.

## 3. Results and Discussion

### 3. 1. Crystal Structure Description

The X-ray single crystal analysis has shown that the NICS-7 compound represents a layered metal-organic framework which crystallizes in a monoclinic space group *Pn* (No. 7). The symmetry independent part of the coordination polymer, depicted in Figure 1, consists of three Mg central ions surrounded by six halves of 4,4'-biphenyldicarboxylate anions (BPDC) and additional four N,N-dimethylformamide molecules (DMF) that complement the coordination spheres of the central Mg ions.

All three Mg ions are surrounded with six octahedrally arranged oxygen atoms. Mg2 is coordinated with

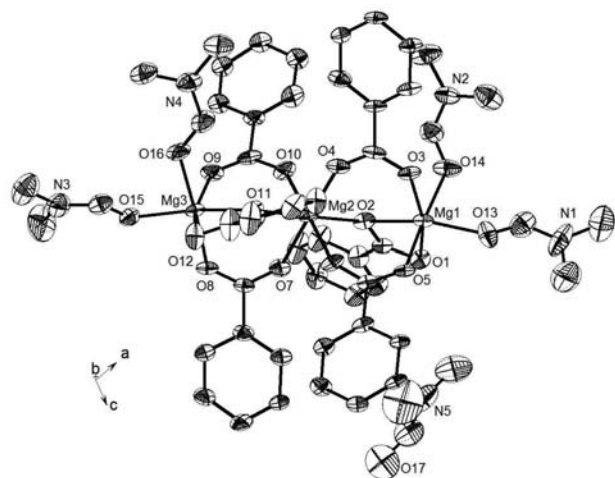


**Figure 1.** ORTEP plot of the NICS-7 asymmetric unit. Hydrogen atoms and atom labels of C are not shown for clarity.

six oxygens from six different BPDC molecules while, on the other hand, Mg1 and Mg3 are surrounded with four oxygens from BPDC and two terminal DMF molecules. When having a closer look at the surroundings of Mg ions, the trimeric secondary building unit (SBU) is observed (Figure 2) in which all three Mg ions lie virtually on the same line (angle Mg1–Mg2–Mg3 is 178.93(16)°) with the interatomic distances Mg1–Mg2 and Mg2–Mg3 of 3.5248(19) and 3.4910(19) Å, respectively. SBU can also be represented as a chain of three MgO<sub>6</sub> octahedra in which the adjacent two octahedra share a common vertex (i.e. atoms O1 and O11 represent the shared vertices).

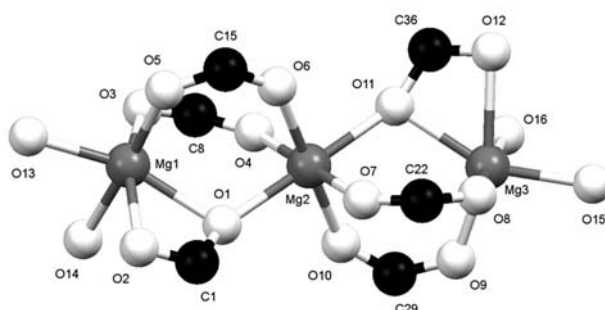


**Figure 2.** Mg-octahedral trimeric secondary building unit in the NICS-7 structure.

A detailed view on SBU also reveals the different binding modes of six symmetry independent BPDC halves: four of them are  $\mu_2$ -bridging ligands while the remaining two are unsymmetrically chelating, i.e. chelating and  $\mu_1$ -bridging at the same time. When taking into account the whole BPDC molecules, two of them are bis bidentate bridging (Figure 3a) while the third is unsymmetrically chelating (Figure 3b); all ligands regardless their binding

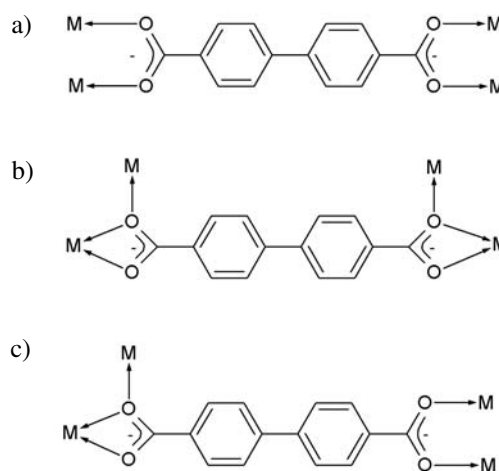


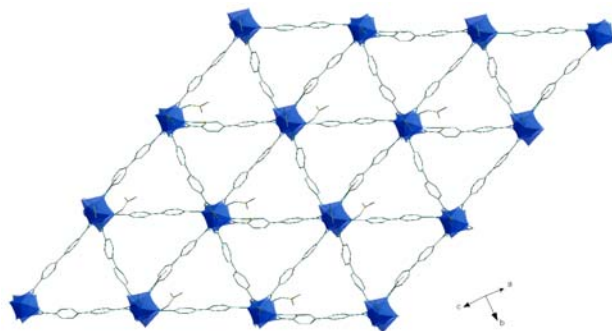
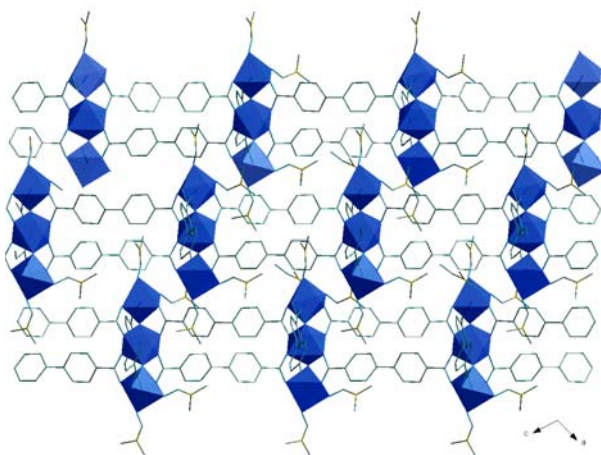
**Figure 3.** The different ligating possibilities of BPDC molecules as found in the NICS-7, (a) bidentate bridging and (b) unsymmetrically chelating. The ligating possibility shown in (c) is not present in NICS-7 but is represented here for the comparison with the related structure - refcode JETZAK<sup>33</sup> (see text).

**Table 2.** Mg–O distances in the first coordination sphere of the title compound.

Bond	Distance [Å]	Bond	Distance [Å]	Bond	Distance [Å]
Mg1–O5	2.018(3)	Mg2–O10	2.024(3)	Mg3–O8	2.012(3)
Mg1–O3	2.058(3)	Mg2–O4	2.030(3)	Mg3–O9	2.038(3)
Mg1–O13	2.066(4)	Mg2–O7	2.038(3)	Mg3–O15	2.049(3)
Mg1–O14	2.114(3)	Mg2–O6	2.038(3)	Mg3–O16	2.105(3)
Mg1–O1	2.151(3)	Mg2–O1	2.091(3)	Mg3–O11	2.144(3)
Mg1–O2	2.187(3)	Mg2–O11	2.100(3)	Mg3–O12	2.249(3)

modes are symmetrical, i.e. the binding mode of both carboxylate groups of the ligand is the same. Distances Mg–O(bridging) are somewhat shorter than Mg–O(chelating); the distance range for the first case is between 2.012(3) and 2.114(3) Å while for the second the distances are between 2.144(3)–2.249(3) Å. Further details on Mg–O distances are collected in Table 2.

Each SBU is surrounded by six BPDC linkers further connected with six adjacent SBUs forming a network of interconnected triangular motifs which eventually form a 2D layer (Figure 4). The basic thickness of the layer can

**Figure 4.** A top-view on a 2D layer of triangles that arise from the connections of adjacent SBUs with organic linkers. MgO<sub>6</sub> units are represented as blue polyhedra.**Figure 5.** The parallel stacking of the 2D layers which run along (101) direction. MgO<sub>6</sub> units are represented as blue polyhedra.

be approximated by the distance between the outermost Mg ions, i.e. Mg1 and Mg3, which is  $\sim 7$  Å. Out of the layer, defined by the length of SBUs, the coordinated DMF molecules are extending. The 2D layers run parallel to (101) direction (Figure 5).

During the crystallographic study we were focused mostly on the structural characteristics of the two-dimensional metal-organic framework whereas the DMF trapped in voids was not addressed although its presence is crucial for the stability of the NICS-7 compound as well as for the stability of related voids-containing structures. From the residual electron density peaks in difference Fourier map it was possible to establish the exact position of only one DMF molecule per asymmetric unit (i.e. two per unit cell), shown on Figure 1. However, further steps of structure refinement procedure have shown several chemically unreasonable Q-peaks whose electron density was removed using *SQUEEZE* routine in *PLATON*<sup>37</sup> which detected two voids in the unit cell, each with volume of approximately 220 Å<sup>3</sup> and each containing 25 electrons. This suggests the presence of additional  $\sim 0.625$  severely disordered molecule of DMF per asymmetric unit or  $\sim 1.25$  DMF per unit cell leading to the final formula of the NICS-7 Mg<sub>3</sub>(BPDC)<sub>3</sub>(DMF)<sub>4</sub>·3.25 DMF, which was also confirmed by TG analysis, described later in the text.

In contrast with the NICS-7, the structure Mg<sub>3</sub>(BPDC)<sub>3</sub>(DMF)<sub>4</sub>·3.8DMF with CCDC refcode JETZAK<sup>33</sup> forms a tridimensional framework with *P2<sub>1</sub>/c* space group symmetry. Surprisingly, at first sight the SBUs of both compounds are the same. Also 2D layers of triangles as seen in Fig. 5 are formed in both structures, and their interconnection in JETZAK leads to the formation of square channels along crystallographic *c* axis. The angles ranges between phenyl rings of the same three symmetry independent BPDC ligands in both compounds are also very similar (ranging from 24.1–43.6° in JETZAK and from 32.4–49.9° in NICS-7) and cannot be the reason for different dimensionalities. But when taking a closer look at three symmetry-independent BPDC ligands, i.e. when taking each one individually into account, the differences that are crucial for different dimensionalities of both coordination polymers can be observed. As already written, in NICS-7 two BPDC ligands are symmetrically ligated in bis-bidentate bridging mode (see Fig. 3a) while the third is unsymmetrically chelating

(Fig. 3b). On the other hand, in JETZAK only one BPDC is symmetrical and bis-bidentate bridging (Fig. 3a) while the remaining two are unsymmetrically bound, with one side bidentate bridging and with the other bidentate chelating and  $\mu_1$ -bridging at the same time (Fig. 3c, i.e. a combination of both coordination modes in NICS-7, shown in Figs. 3a and 3b).

NICS-7 compound was also structurally characterized by FT-IR spectroscopy in order to evaluate the nature of connectivity of DMF molecules. FT-IR spectrum of NICS-7 compound is shown on Figures 6 on two separate wavenumber regions in order to better resolve important bands. In the wavenumber region between 2500 and 3600  $\text{cm}^{-1}$  (Figure 7a) two sharp bands at 3064 and 2932  $\text{cm}^{-1}$  are assigned to C-H symmetric vibrations in methyl groups of DMF. Broad band with the peak at approximately 3300  $\text{cm}^{-1}$ , typical for hydrogen-bonded –OH group vibrations, is very weak in intensity. This could imply that water is present in the sample only in traces, most probably as moisture physisorbed on the surface of the mate-

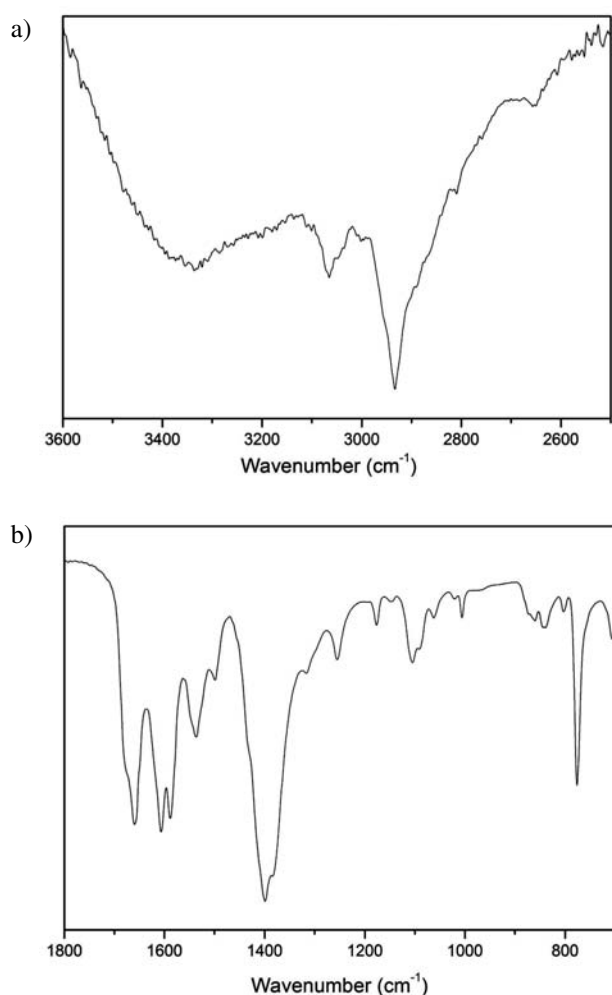


**Figure 6.** FT-IR spectra of the NICS-7 material shown at (a) higher and (b) lower wavenumber regions.

rial and it is not part of the structure. FT-IR spectrum in the lower wavenumbers region (900–1800  $\text{cm}^{-1}$ ) is shown in Figure 7b. The spectrum exhibits some characteristic bands which are in agreement with the described structure. Strong bands at 1600 and 1400  $\text{cm}^{-1}$  are assigned to C-C vibrations of aromatic ring. The absence of the band in the range between 1680 and 1800  $\text{cm}^{-1}$  indicates the presence of only deprotonated carboxylic groups. Intense band with the peak at 1659  $\text{cm}^{-1}$  and clearly visible shoulder at slightly higher wavenumbers are assigned to C=O stretching of the DMF molecule. These two overlapping bands indicate that DMF molecules occur within the structure in two environments, one part being coordinated to Mg centres and the other located within the structure in free mode.<sup>39</sup> This findings are in agreement to crystal structure features.

### 3. 2. Thermal Properties

Thermogravimetric analysis shown on Figure 7 indicates complexity in weight loss process occurring in several overlaid steps in broad temperature range from room temperature up to 400 °C. Even though DMF molecules are located in two different environments in the NICS-7 structure (coordinative DMF and free DMF trapped between the  $\text{Mg}_3(\text{BPDC})_3(\text{DMF})_4$  layers) its removal is not straightforward and does not occur in two distinctive steps. Nevertheless, the dynamics of DMF removal during heating can still be deduced. First weight loss up to 100 °C should be due to the removal of free DMF located in the voids of the NICS-7 structure. Weight loss of about 15 wt.% is in accordance with findings from single-crystal structure analysis. Remaining, coordinated DMF is removed in broad temperature range from 100 to 400 °C. Its weight loss of approximately 23 wt.% is in agreement with theoretical values considering the NICS-7 formula,  $\text{Mg}_3(\text{BPDC})_3(\text{DMF})_4 \cdot 3.25\text{DMF}$  (21.9 wt.%). Removal of free DMF seems to cause the collapse of the Mg-BPDC layers leading to partial blocking of voids and preventing the unobstructed removal of coordinative DMF from the material. Only cracking of the crystals occurring at higher temperatures allows the removal of all DMF from the material. Thermal properties were additionally characterized by temperature-programmed XRD analysis. As it is indicated from TP-XRD patterns recorded up to 600 °C (Figure 8), the structure of NICS-7 remains stable only up to 50 °C. At higher temperatures, the removal of free DMF molecules causes significant loss of structure integrity resulting in formation of amorphous Mg-BPDC phase and already partial formation of magnesium oxide. As it was already assumed by X-ray structure and TG analyses, DMF located between the layers of  $\text{Mg}_3(\text{BPDC})_3(\text{DMF})_4$  has significant role in keeping the crystal structure stable at room temperature. Even more, the structure seem to be stable only with DMF inclusions within the voids. An attempt to exchange

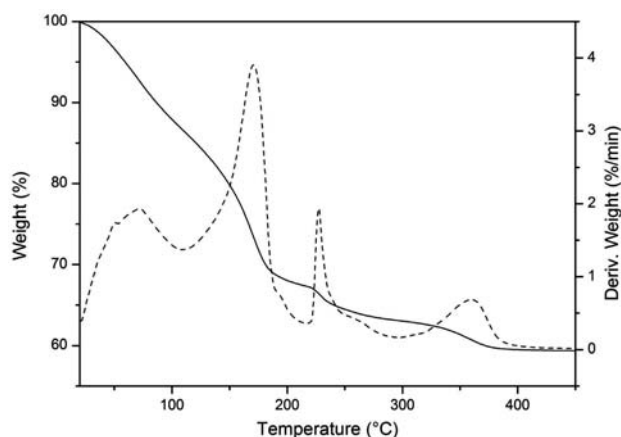


**Figure 7:** TG (solid line) and DTG (dashed line) curves of NICS-7 material.

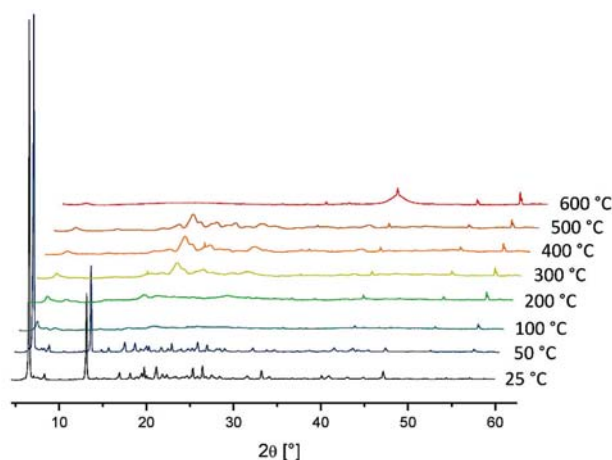


**Figure 8:** Temperature-programmed XRD patterns of NICS-7 material recorded at given temperatures.

DMF with water, methanol or acetonitrile was unsuccessful and led to the collapse of structure upon exposure to these solvent molecules at room temperature.

## 4. Conclusions

In this contribution we present the synthesis, crystal structure and thermal properties of new magnesium 4,4'-biphenyldicarboxylate MOF-type material denoted as NICS-7. Inorganic building unit consists of three linearly arranged  $\text{MgO}_6$  octahedra with common vertices in which terminal Mg atoms from trimeric clusters are coordinated not only with BPDC ligands but also by DMF molecules. Inorganic SBUs are connected through BPDC ligands via bidentate bridging and unsymmetrically chelating modes forming layers of  $\text{Mg}_3(\text{BPDC})_3(\text{DMF})_4$ . Between layers additional free DMF molecules are located: the positions of two per formula unit are established while the rest 1.25

are heavily disordered. These DMF molecules have a crucial role on keeping the whole NICS-7 structure stable. As it was indicated by TG analysis and temperature-programmed XRD, the removal of un-coordinated DMF moieties, which occurs at 100 °C, causes severe loss of structure integrity and formation of amorphous Mg-BPDC phase.

## 5. References

1. H. Furukawa, K. E. Cordova, M. O'Keeffe, O. M. Yaghi, *Science* **2013**, *341*, 1230444.
2. M. Ranocchiari, J. A. van Bokhoven, *Phys. Chem. Chem. Phys.* **2011**, *13*, 6388–6396.
3. P. Horcajada, R. Gref, T. Baati, P. K. Allan, G. Maurin, P. Couvreur, G. Férey, R. E. Morris, Serre, C. *Chem. Rev.* **2012**, *112*, 1232–1268.
4. A. Morozan, F. Jaouen, *Energy Environ. Sci.* **2012**, *5*, 9269–9290.
5. M. Gaab, N. Trukhan, S. Maurer, R. Gummaraju, U. Müller, *Microporous Mesoporous Mater.* **2012**, *157*, 131–136.
6. O. K. Farha, J. T. Hupp, *Acc. Chem. Res.* **2010**, *43*, 1166–1175.
7. H. Li, M. Eddaoudi, M. O'Keeffe, O. M. Yaghi, *Nature* **1999**, *402*, 276–279.
8. S. M. Cohen, *Chem. Rev.* **2012**, *112*, 970–1000.
9. R. B. Getman, Y.-S. Bae, C. E. Wilmer, R. Q. Snurr, *Chem. Rev.* **2011**, *112*, 703–323.
10. J.-R. Li, R. J. Kuppler, H.-C. Zhou, *Chem. Soc. Rev.* **2009**, *38*, 1477–1504.
11. R. E. Morris, P. S. Wheatley, *Angew. Chem. Int. Ed.* **2008**, *47*, 4966–4981.
12. J. A. Rood, B. C. Noll, K. W. Henderson, *Inorg. Chem.* **2006**, *45*, 5521–5528.
13. A. Mesbah, L. Aranda, J. Steinmetz, E. Rocca, M. François, *Solid State Sci.* **2011**, *13*, 1438–1442.
14. Z. Hulvey, A.K. Cheetham, *Solid State Sci.* **2007**, *9*, 137–143.
15. J. A. Rood, W. C. Boggess, B. C. Noll, K.W. Henderson, *J. Am. Chem. Soc.* **2007**, *129*, 13675–13682.
16. J. Zhang, S. Chen, H. Valle, M. Wong, C. Austria, M. Cruz, X. Bu, *J. Am. Chem. Soc.* **2007**, *129*, 14168–14169.
17. M. Dincă, J. R. Long, *J. Am. Chem. Soc.* **2005**, *127*, 9376–9377.
18. Z. Guo, G. Li, L. Zhou, S. Su, Y. Lei, S. Dang, H. Zhang, *Inorg. Chem.* **2009**, *48*, 8069–8071.
19. Y. E. Cheon, J. Park, M. P. Suh, *Chem. Commun.* **2009**, 5436–5438.
20. B. Schmitz, I. Krkljus, E. Leung, H. W. Höffken, U. Müller, M. Hirscher, *ChemSusChem* **2010**, *3*, 758–761.
21. A. Mallick, S. Saha, P. Pachfule, S. Roy, R. Banarjee, *J. Mater. Chem.* **2010**, *20*, 9073–9080.
22. K. Sumida, C. M. Brown, Z. R. Herm, S. Chavan, S. Bordiga, J. R. Long, *Chem. Commun.* **2011**, *47*, 1157–1159.
23. Z. Bao, S. Alnemrat, L. Yu, I. Vasiliev, Q. Ren, X. Lu, S. Deng, *Langmuir* **2001**, *27*, 13554–13562.
24. C. Volkringer, T. Loiseau, J. Marrot, G. Férey, *CrystEngComm.* **2009**, *11*, 58–60.

25. K. Jayaramulu, P. Kanoo, S. J. George, T. K. Maji, *Chem. Commun.* **2010**, 46, 7906–7908.
26. P. D. C. Dietzel, R. Bloom, H. Fjellvåg, *Eur. J. Inorg. Chem.* **2008**, 23, 3624–3632.
27. R. P. Davies, R. J. Less, P. D. Lickiss, A. J. P. White, *Dalton Trans.* **2007**, 2528–2535.
28. C. A. Williams, A. J. Blake, C. Wilson, P. Hubberstey, M. Schröder, *Cryst. Growth Design* **2008**, 8, 911–922.
29. I. Senkowska, S. Kaskel, *Eur. J. Inorg. Chem.* **2006**, 22, 4564–4569.
30. D. Banarjee, J. Finkelstein, A. Smirnov, P. M. Forster, L. A. Borkowski, S. J. Teat, J. B. Parise, *Cryst. Growth Design* **2011**, 11, 2572–2579.
31. M. Mazaj, T. Birsa Čelič, G. Mali, M. Rangus, V. Kaučič, N. Zabukovec Logar, *Cryst. Growth Design* **2013**, 13, 3825–3834.
32. H.-K. Liu, X.-W. Peng, C.-H. Lin, *Acta Cryst. E* **2009**, 65, m237.
33. J. A. Rood, B. C. Noll, K. W. Henderson, *Main Group Chem.* **2006**, 5, 21–30.
34. Oxford Diffraction (2011). CrysAlis PRO. Oxford Diffraction Ltd, Yarnton, Oxfordshire, England.
35. A. Altomare, M. C. Burla, M. Camalli, G. L. Casciarano, C. Giacovazzo, A. Guagliardi, A. G. G. Moliterni, G. Polidori, R. Spagna, *J. Appl. Cryst.* **1999**, 32, 115–119.
36. G. M. Sheldrick, *Acta Cryst.* **2008**, A64, 112–122.
37. A. L. Spek, *J. Appl. Crystallogr.* **2003**, 36, 7–13.
38. L. J. Farrugia, *J. Appl. Crystallogr.* **1997**, 30, 565–565.
39. M. Mazaj, G. Mali, M. Rangus, E. Žunkovič, S. Kaučič, N. Zabukovec Logar, *J. Phys. Chem. C.* **2013**, 117, 7552–7564.

## Povzetek

Nov magnezijev 4,4'-bifenildikarboksilat (BPDC) smo solvotermalno sintetizirali v prisotnosti DMF. Kristalna struktura s formulo  $\text{Mg}_3(\text{BPDC})_3(\text{DMF})_4$  in oznako NICS-7, je bila rešena v monoklinski simetriji s prostorsko skupino  $Pn$  (št. 7) in parametric osnovne celice  $a = 12.6433(7) \text{ \AA}$ ,  $b = 13.3950(5) \text{ \AA}$ ,  $c = 19.9230(8) \text{ \AA}$ ,  $\beta = 107.131(5)^\circ$ . Strukturo sestavljajo linearni trimeri  $\text{MgO}_6$  oktaedrov s skupnimi oglišči, ki so preko BPDC ligandov povezane v 2-dimenzionalno plastovito hibridno ogrodje. Vsak od terminalnih Mg atomov znotraj trimernih enot je koordiniran z dvema molekulama DMF. Plasti  $\text{Mg}_3(\text{BPDC})_3(\text{DMF})_4$  so stabilizirane s prostimi molekulami DMF, ki se v odprtinah med plastmi nahajajo v kristalografsko neurejeni obliki. Termične lastnosti NICS-7 smo določili s TG and temperaturno-programirano XRD analizo. Struktura ostane stabilna le do  $50^\circ\text{C}$ . Odstranitev DMF molekul, do katerega pride pri višjih temperaturah, povzroči sesedanje plasti in nastanek amorfne Mg-BPDC faze.